Symmetry energy effects on the mixed hadron-quark phase at high baryon density

M. Di Toro,[1,2,*] B. Liu,[3,4] V. Greco,[1,2] V. Baran,[5] M. Colonna,[1] and S. Plumari[1,2]
[1]*Laboratori Nazionali del Sud INFN, I-95123 Catania, Italy*
[2]*Physics and Astronomy Department, University of Catania*
[3]*IHEP, Chinese Academy of Sciences, Beijing, China*
[4]*Theoretical Physics Center for Scientific Facilities, Chinese Academy of Sciences, 100049 Beijing, China*
[5]*Physics Faculty, University of Bucharest and NIPNE-HH, Romania*
(Received 5 July 2010; revised manuscript received 10 September 2010; published 28 January 2011)

The phase transition of hadronic to quark matter at high baryon and isospin density is analyzed. Relativistic mean-field models are used to describe hadronic matter, and the MIT bag model is adopted for quark matter. The boundaries of the mixed phase and the related critical points for symmetric and asymmetric matter are obtained. Due to the different symmetry term in the two phases, isospin effects appear to be rather significant. With increasing isospin asymmetry the binodal transition line of the (T, ρ_B) diagram is lowered to a region accessible through heavy-ion collisions in the energy range of the new planned facilities (e.g., the FAIR/NICA projects). Some observable effects are suggested, in particular an isospin distillation mechanism with a more isospin asymmetric quark phase, to be seen in charged meson yield ratios, and an onset of quark number scaling of the meson-baryon elliptic flows. The presented isospin effects on the mixed phase appear to be robust with respect to even large variations of the poorly known symmetry term at high baryon density in the hadron phase. The dependence of the results on a suitable treatment of isospin contributions in effective QCD Lagrangian approaches, at the level of explicit isovector parts and/or quark condensates, is discussed.

DOI: 10.1103/PhysRevC.83.014911 PACS number(s): 21.65.Mn, 21.65.Ef, 25.75.Nq, 05.70.Ce

I. INTRODUCTION

Several suggestions are already present about the possibility of interesting isospin effects on the transition to a mixed hadron-quark phase at high baryon density [1–3]. This seems to be a very appealing physics program for the new facilities FAIR at GSI-Darmstadt [4] and NICA at JINR-Dubna [5], where heavy-ion beams (even unstable, with large isospin asymmetry) will be available with good intensities in the 1–30 *A* GeV energy region.

The weak point of those predictions is the lack of a reliable equation of state (EoS) that can describe in a consistent way the two phases, hadronic and deconfined, at high baryon density. In particular none of the two-EoS models obviously can reproduce continuous transitions, such as second-order phase transitions or crossovers. However, they can be useful to check if we can have a first-order transition at lower temperatures. In the latter case, while we cannot localize the corresponding critical end point, we can study with some confidence the properties of the mixed-phase region if realistic effective interactions in the two phases are used. Such discussion will also lead to a strong motivation to work on more refined effective theories for strong interacting matter. The aim of our paper is to show our results, on the dependence on the EoS choices in the two phases and on possible observables, that would further stimulate the search in the field, in theory as well as in experiment.

Isospin effects on the transition are ruled by the symmetry term in the two phases. For the hadronic side in all the two-EoS approaches, so far mostly applied to develop hybrid models for neutron stars, a rather strong density dependence of the symmetry energy has been used [1–3,6–11]. This point however is still open mainly due to the present lack of good data for isospin effects on heavy-ion collisions at intermediate energies, in particular on collective flows and particle productions [12–17]. Here we extend our study also to cases with a much softer hadronic symmetry term in order to check the "robustness" of the expected isospin effects.

For the quark matter MIT bag [18], in Refs. [1–3,6–8], or Nambu–Jona-Lasinio (NJL) [19,20], in Refs. [9–11], models have been adopted, always without explicit isospin-dependent contributions. Here we also mainly used standard MIT bag models, but we also discuss the consequence of some isospin effects in NJL approaches and possible indirect corrections due to the color-pairing residual interaction [21].

We finally like to note that the isospin-dependence predictions can also be used in the opposite way: If we see such isospin effects on the sensitive observables suggested here we can get more confidence on the reliability of the used equations of state in the two phases.

This is the plan of the paper. In Sec. I we present a simple motivation for a first-order transition with isospin effects. In Sec. II the procedure to construct the "binodal surface" from the Gibbs conditions is presented, with particular attention to the physical interpretation of the observed end point. Properties of the mixed phase are evaluated in Sec. III, using different density-dependent symmetry terms for the hadron sector. Section IV is devoted to the introduction of isospin contributions in the quark effective EoS. Sensitive observables in collisions of neutron-rich ions at intermediate energies are suggested in Sec. V, with relative perspectives. Finally, we present details of the effective hadron interactions used in Appendix A and of the isospin-dependent extension of the NJL model discussed in the paper in Appendix B.

*ditoro@lns.infn.it

II. THE REASON FOR A FIRST-ORDER TRANSITION WITH ISOSPIN EFFECTS

The main qualitative argument in favor of a first-order hadron-quark transition at high density and low temperature, with noticeable isospin effects, can be derived from Fig.1. Here we compare typical equations of state for hadron (nucleon) and quark matter, at zero temperature, for symmetric [$\alpha \equiv (\rho_n - \rho_p)/\rho_B \equiv -\rho_3/\rho_B = 0.0$] and neutron matter ($\alpha = 1.0$), where $\rho_{n,p}$ are the neutron and proton densities and $\rho_B = \rho_n + \rho_p$ is the total baryon density.

In this first simple calculation, a kind of "homework," for the hadron part we use a relativistic mean-field (RMF) EoS ([12,22,23]) with nonlinear terms and an effective ρ-meson coupling for the isovector part, largely used to study isospin effects in relativistic heavy-ion collisions [3,12]. However, in the paper we will probe several effective hadron interactions to check the "robustness" of the observed symmetry energy effects. In order to keep a smooth flow of the physics points in the discussion, details about the adopted effective nucleon-meson Lagrangians are presented in Appendix A.

The energy density and the pressure for the quark phase are given by the MIT bag model [18] (two-flavor case) and read, respectively,

$$\epsilon = 3 \times 2 \sum_{q=u,d} \int \frac{d^3k}{(2\pi)^3} \sqrt{k^2 + m_q^2} (f_q + \bar{f}_q) + B, \quad (1)$$

$$P = \frac{3 \times 2}{3} \sum_{q=u,d} \int \frac{d^3k}{(2\pi)^3} \frac{k^2}{\sqrt{k^2 + m_q^2}} (f_q + \bar{f}_q) - B, \quad (2)$$

where B denotes the bag constant (the bag pressure), taken as a rather standard value from the hadron spectra ($B = 85.7$ MeV fm^{-3}, with no density dependence), m_q are the quark masses ($m_u = m_d = 5.5$ MeV), and f_q and $\bar{f}_q$ represent the Fermi distribution functions for quarks and antiquarks. The quark number density is given by

$$\rho_i = \langle q_i^+ q_i \rangle = 3 \times 2 \int \frac{d^3k}{(2\pi)^3} (f_i - \bar{f}_i), \quad i = u, d. \quad (3)$$

The transition to the more repulsive quark matter will appear around the crossing points of the two equations of state We see that such crossing for symmetric matter ($\alpha_H = \alpha_Q = 0.0$) is located at rather high density, $\rho_B \simeq 7\rho_0$, while for pure neutron matter ($\alpha_H = \alpha_Q = 1.0$) it decreases to about $3\rho_0$. Of course Fig. 1 represents just a simple energetic argument to support the hadron-quark transition to occur at lower baryon densities for more isospin asymmetric matter. In the rest of the paper we will rigorously consider the case of a first-order phase transition in the Gibbs frame for a system with two conserved charges (baryon and isospin), in order to derive more detailed results. Since the first-order phase transition presents a jump in energy, we can expect the mixed phase to start at densities even before the crossing points of Fig. 1. The lower boundary then can be predicted at relatively low baryon densities for asymmetric matter, likely reached in relativistic heavy-ion collisions. Moreover, this point is certainly of interest for the structure of the crust and the inner core of neutron stars (e.g., see Refs. [6–11] and the review [24]). We remark that in Ref. [6] similar results are obtained with rather different hadronic approaches, the RMF and the nonrelativistic Brueckner-Hartree-Fock (BHF) theory.

We finally note that these conclusions are rather independent of the isoscalar part of the used hadron EoS at high density, which is chosen to be rather soft, in agreement with collective flow and kaon production data [25,26].

In the bag model used no *residual* gluon interactions, the α_s strong coupling parameter, are included. We remark that this in fact would enhance the above effect, in the direction of overall lower transition densities, since it represents an attractive correction for a fixed B constant (see [27]). A reduction of the bag constant with increasing baryon density, as suggested by various models (see Ref. [6]) will also go in the direction of an "earlier" (lower density) transition, as already seen in Ref. [2]. At variance, the presence of explicit isovector contributions in the quark phase could play an important role, as shown in the following also for other isospin properties inside the mixed phase.

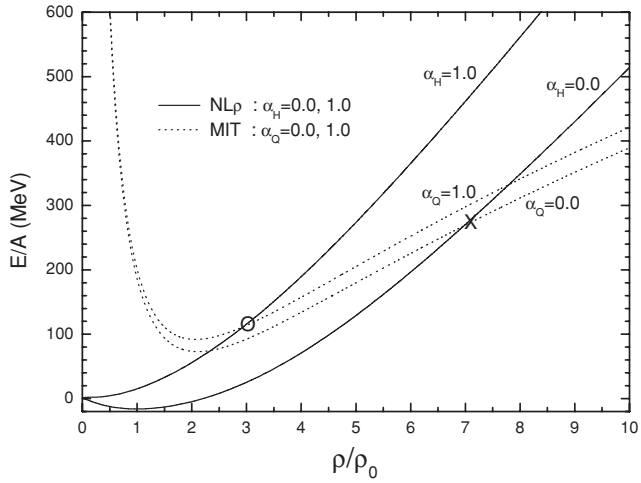

FIG. 1. Zero-temperature EoS of symmetric neutron matter: hadron (NLρ; solid lines) vs quark (MIT bag; dashed lines). $\alpha_{H,Q}$ represent the isospin asymmetry parameters of, respectively, hadron and quark matter: $\alpha_{H,Q} = 0$, symmetric matter; $\alpha_{H,Q} = 1$, neutron matter.

III. ISOSPIN EFFECTS ON THE MIXED PHASE

We can study in detail the isospin dependence of the transition densities [1–3]. The structure of the mixed phase is obtained by imposing the Gibbs conditions [28] for chemical potentials and pressure and by requiring the conservation of the total baryon and isospin densities:

$$\begin{aligned} \mu_B^H(\rho_B^H, \rho_3^H, T) &= \mu_B^Q(\rho_B^Q, \rho_3^Q, T), \\ \mu_3^H(\rho_B^H, \rho_3^H, T) &= \mu_3^Q(\rho_B^Q, \rho_3^Q, T), \\ P^H(T)(\rho_B^H, \rho_3^H, T) &= P^Q(T)(\rho_B^Q, \rho_3^Q, T), \\ \rho_B &= (1-\chi)\rho_B^H + \chi\rho_B^Q, \\ \rho_3 &= (1-\chi)\rho_3^H + \chi\rho_3^Q, \end{aligned} \quad (4)$$

where χ is the fraction of quark matter in the mixed phase and T is the temperature.

The consistent definitions for the densities and chemical potentials in the two phases are given by

$$\rho_B^H = \rho_p + \rho_n, \quad \rho_3^H = \rho_p - \rho_n,$$
$$\mu_B^H = \frac{\mu_p + \mu_n}{2}, \quad \mu_3^H = \frac{\mu_p - \mu_n}{2} \tag{5}$$

for the hadron phase and

$$\rho_B^Q = \tfrac{1}{3}(\rho_u + \rho_d), \quad \rho_3^Q = \rho_u - \rho_d,$$
$$\mu_B^Q = \tfrac{3}{2}(\mu_u + \mu_d), \quad \mu_3^Q = \frac{\mu_u - \mu_d}{2} \tag{6}$$

for the quark phase.

The related asymmetry parameters are

$$\alpha^H \equiv -\frac{\rho_3^H}{\rho_B^H} = \frac{\rho_n - \rho_p}{\rho_n + \rho_p}, \quad \alpha^Q \equiv -\frac{\rho_3^Q}{\rho_B^Q} = 3\frac{\rho_d - \rho_u}{\rho_d + \rho_u}. \tag{7}$$

Nucleon and quark chemical potentials, as well as the pressures in the two phases, are directly derived from the respective equations of state.

In this way we get the *binodal* surface which gives the phase coexistence region in (T, ρ_B, ρ_3) space. For a fixed value of the total asymmetry $\alpha_T = -\rho_3/\rho_B$ we will study the boundaries of the mixed-phase region in the (T, ρ_B) plane. Since in general the charge chemical potential is related to the symmetry term of the EoS [12], $\mu_3 = 2E_{\rm sym}(\rho_B)\frac{\rho_3}{\rho_B}$, we expect critical and transition densities to be rather sensitive to the isovector channel in the two phases.

In the hadron sector we will use nonlinear relativistic mean-field models [3,12,23], with different structure of the isovector part, already tested to describe the isospin dependence of collective flows and meson production for heavy-ion collisions at intermediate energies [29–31]. We will refer to these different iso-Lagrangians as (i) NL, where no isovector meson is included and the symmetry term is only given by the kinetic Fermi contribution, (ii) NLρ when the interaction contribution of an isovector-vector meson is considered, and (iii) NL$\rho\delta$ where also the contribution of an isovector-scalar meson is accounted for. See details in Appendix A1 and Refs. [3,12,23].

We will look at the effect on the hadron-quark transition of the different stiffnesses of the symmetry term at high baryon densities in the different parametrizations. As clearly shown in Appendix A1, where a rather transparent form for the density dependence of the symmetry energy in RMF approaches is discussed, the potential part of the symmetry term will be proportional to the baryon density in the NLρ choice and will be even stiffer in the NL$\rho\delta$ case.

We are well aware that there are several uncertainties on the stiffness of the symmetry energy at high baryon density, mainly due to the lack of suitable data (see the reviews [12,14]). Therefore in the next section we will also show results with effective hadron interactions based on RMF models with density-dependent meson-nucleon couplings (density-dependent relativistic hadron forces; Appendix A2) that present much softer symmetry terms at high baryon density. In this way we can directly check the "stability" of the observed isospin effects on the mixed phase.

As already mentioned, in the quark phase we use the MIT bag model, where the symmetry term is given only by the Fermi contribution. The bag parameter B is fixed for each baryon density to a constant, rather standard, value $B^{1/4} = 160$ MeV, corresponding to a bag pressure of 85.7 MeV fm^{-3}.

In general for each effective interactive Lagrangian we can simulate the solution of the highly nonlinear system of Eqs. (4) via an iterative minimization procedure, in order to determine the binodal boundaries.

A relatively simple calculation can be performed at zero temperature. The isospin effect (asymmetry dependence) on the lower ($\chi = 0.0$) and upper ($\chi = 1.0$) transition densities of the mixed phase are shown in Fig. 2 for various choices of the hadron EoS. The effect of a larger repulsion of the symmetry energy in the hadron sector, from NL to NLρ and to NL$\rho\delta$, is clearly evident on the lower boundary with a sharp decrease of the transition density even at relatively low asymmetries.

Typical results for isospin effects on the whole binodal "surface" are presented in Fig. 3 for symmetric and asymmetric matter. For the hadron part we have started from an NLρ effective Lagrangian very close to other widely used relativistic effective models, e.g., see the GM3 model of Ref. [32] and the NL3 interaction of Ring and collaborators [33], which has also given good nuclear structure results, even for exotic nuclei.

As expected, the lower boundary of the mixed phase is mostly affected by isospin effects. In spite of the relatively small total asymmetry, $\alpha = 0.2$, we clearly observe in Fig. 3 a shift to the left of the first transition boundary, in particular at low temperature.

In the symmetric matter case the mixed phase is evaluated from the simpler Maxwell conditions. The results are shown in Fig. 4 for the same hadron and quark equations of state as in Fig. 3 at temperatures $T = 0$, 50, and 80 MeV. The equal chemical potential densities (intersection of the dotted line in the lower panel) must correspond to the equal pressure densities of the upper panels. We see that at $T = 0$ MeV the mixed phase is nicely centered around $\rho/\rho_0 \simeq 7.0$, exactly

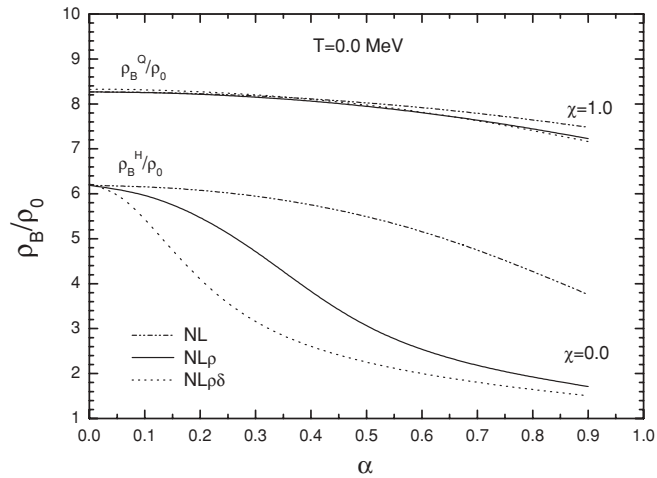

FIG. 2. Dependence on the hadron symmetry energy of the lower ($\chi = 0.0$) and upper ($\chi = 1.0$) boundaries of the mixed phase, at zero temperature, vs the asymmetry parameter. Quark EoS: MIT bag model with $B^{1/4} = 160$ MeV.

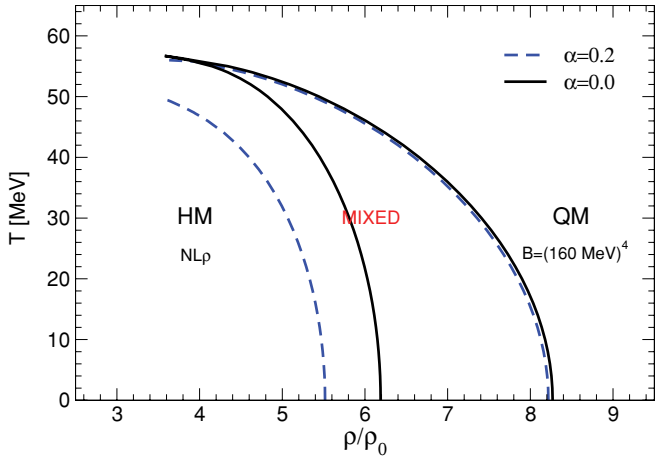

FIG. 3. (Color online) Binodal surface for symmetric ($\alpha = 0.0$) and asymmetric ($\alpha = 0.2$) matter. Hadron EoS from NLρ interaction. Quark EoS: MIT bag model with $B^{1/4} = 160$ MeV.

the $\alpha = 0$ crossing point of Fig. 1, confirming our energetic argument about the transition location. The two boundaries are precisely at $\rho_H/\rho_0 = 6.2$ and $\rho_Q/\rho_0 = 8.3$ at a chemical potential $\mu = 1597.0$ MeV.

From Fig. 4 we also see that the size of the mixed phase is shrinking with temperature; it is very narrow at $T = 50$ MeV and finally at $T = 80$ MeV we no longer can have a first-order transition. In fact a kind of critical end point is appearing at $T_c \simeq 58$ MeV, $\rho_c/\rho_0 \simeq 3.8$, $P_c \simeq 120$ MeV/ fm^3, and $\mu_c \simeq 1090$ MeV (see also Fig. 3). The result is dependent on the choice of the bag constant, with an increase of the critical temperature with the bag value due to the reduction of the pressure in the quark phase, while the chemical potentials are not affected.

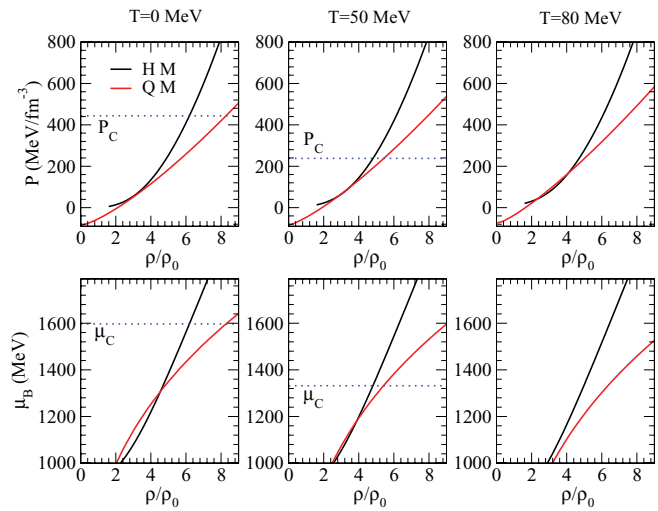

FIG. 4. (Color online) Maxwell construction for symmetric ($\alpha = 0.0$) matter at temperatures $T = 0$, 50, and 80 MeV. The dashed lines correspond to the coexistence values of pressure (upper panels) and chemical potential (lower panels). Hadron EoS (black curves) from NLρ interaction; quark EoS (gray curves) from MIT bag model with $B^{1/4} = 160$ MeV.

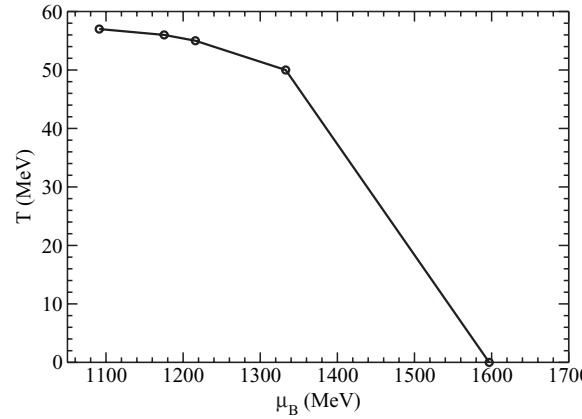

FIG. 5. Phase transition line in the (T, μ) plane for symmetric ($\alpha = 0.0$) matter. Hadron and quark equations of state are as in Fig. 4.

However, as already noted in Sec. I, within the present two-EoS approach it is impossible to discuss the nature of the transition around this apparent critical end point. The fact that we reach a point with equal densities in the two phases is not implying the onset of a continuous transition. Indeed from the coexistence conditions of a first-order transition we can have a point with equal densities but with a gap in the entropy densities. Since we can follow the transition in the (T, μ) plane, such a point will correspond to a zero of $dT/d\mu$, from the Clausius-Clapeyron equation.

We have checked this possibility for the transition discussed before (see Fig. 4) of symmetric matter. In Fig. 5 we present the calculated points of the phase diagram in the (T, μ) plane. We see that approaching the end point of the binodal surface we come very close to the $dT/d\mu = 0$ condition and so we cannot deduce that we have reached a real critical end point of the first-order transition.

We note that this result is not implying that the properties of the mixed phase at lower temperatures discussed within two-EoS models are meaningless. We can trust them if we are using "realistic" effective interactions in the two phases. In fact, this is the main point raised here, where the focus is on the isospin dependence of the mixed phase at low temperature, which can be probed in heavy-ion collisions at intermediate energies.

IV. INSIDE THE MIXED PHASE OF ASYMMETRIC MATTER

For $\alpha = 0.2$ asymmetric matter, in Figs. 6 and 7 we show also the (T, ρ_B) curves inside the mixed phase corresponding to 20% and 50% presence of the quark component ($\chi = 0.2, 0.5$), evaluated respectively with the two choices, NLρ and NL$\rho\delta$, of the symmetry interaction in the hadron sector. We note, as also expected from Fig. 2, that in the more repulsive NL$\rho\delta$ case the lower boundary is notably shifted to the left. However, this effect is not so evident for the curve corresponding to a 20% quark concentration, and it is almost absent for the 50% case. The conclusion seems to be that for a stiffer symmetry term in a heavy-ion collision at intermediate energies during the compression stage we can have a greater

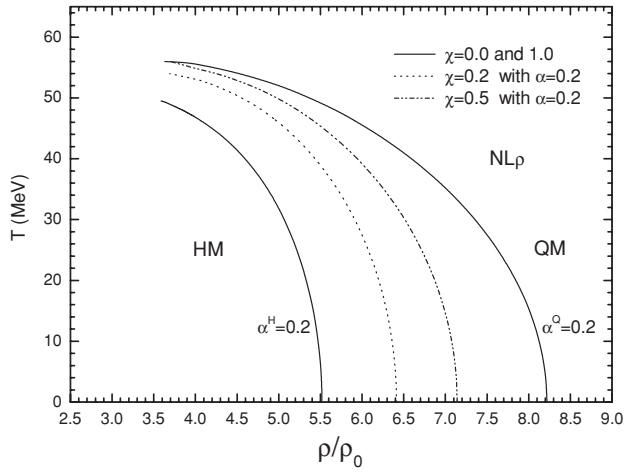

FIG. 6. Asymmetric $\alpha = 0.2$ matter. Binodal surface and (T, ρ_B) curves for various quark concentrations ($\chi = 0.2, 0.5$) in the mixed phase. Quark EoS: MIT bag model with $B^{1/4} = 160$ MeV; hadron EoS: NLρ effective interaction.

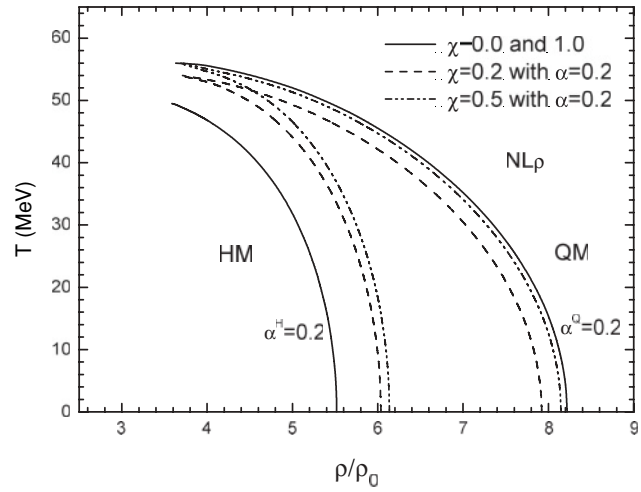

FIG. 8. Asymmetric $\alpha = 0.2$ matter. Binodal surface and (T, ρ_B^H, ρ_B^Q) curves for various quark concentrations in the mixed phase. Quark EoS: MIT bag model with $B^{1/4} = 160$ MeV; hadron EoS: NLρ effective interaction.

chance of probing the mixed phase, although in a region with small weight of the quark component.

In fact, from the solution of the system (4) we get the baryon densities ρ_B^H, ρ_B^Q in the two phases for any χ value. In Figs. 8 and 9 we present the results for the same weights (20% and 50%) of the quark phase of the previous figures. The quark phase appears always with larger baryon density, even for the lowest value of the concentration.

Can we expect some signatures related to the subsequent hadronization in the following expansion?

An interesting possibility comes from the study of the asymmetry α^Q in the quark phase. In fact, since the symmetry energy is rather different in the two phases we can expect an isospin distillation (or fractionation), very similar to the one observed in liquid-gas transition in dilute nuclear matter [12,34,35], this time with the larger isospin content in the higher density quark phase.

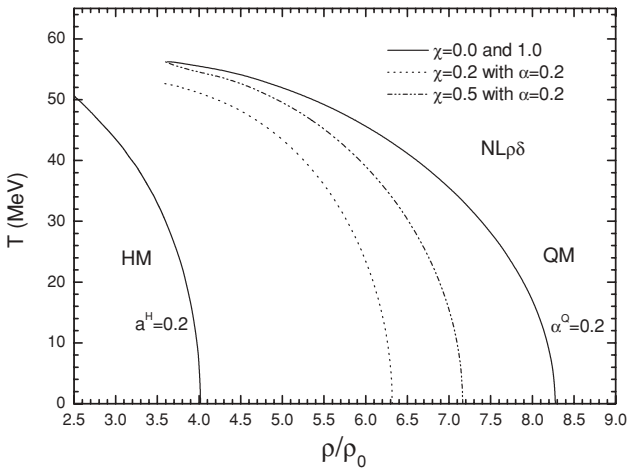

FIG. 7. Same as in Fig. 6, but for the NL$\rho\delta$ effective interaction in the hadron sector.

In Fig. 10 we show the asymmetry α^Q in the quark phase as a function of the quark concentration χ for the case with global asymmetry $\alpha = 0.2$ (zero temperature). The calculation is performed with the two choices of the symmetry term in the hadron sector. We see an impressive increase of the quark asymmetry when we approach the lower boundary of the mixed phase, even to values larger than one, likely just for numerical accuracy.[1] Of course the quark asymmetry recovers the global value 0.2 at the upper boundary $\chi = 1$. A simple algebraic calculation allows us to evaluate the corresponding asymmetries of the hadron phase. In fact, from charge conservation we have that for any χ mixture the global asymmetry α is given by

$$\alpha \equiv -\frac{\rho_3}{\rho_B} = \frac{(1-\chi)\alpha^H}{(1-\chi)+\chi\frac{\rho_B^Q}{\rho_B^H}} + \frac{\chi\alpha^Q}{(1-\chi)\frac{\rho_B^H}{\rho_B^Q}+\chi}. \quad (8)$$

For any χ, from the calculated α^Q of Fig. 10 and the ρ_B^H and ρ_B^Q values of Figs. 8 and 9, we can get the correspondent asymmetry of the hadron phase α^H. For a 20% quark concentration we have an α^Q/α^H ratio of around 5 for NLρ and around 20 for NL$\rho\delta$, being more repulsive in the isovector channel. It is also interesting to compare the isospin content N/Z of the high-density region expected from transport simulations without the hadron-quark transition and

[1] In principle there is nothing wrong with $\alpha^Q > 1$ evaluations (although we note that for pure neutron matter the quark phase asymmetry should be 1, since $\rho_d = 2\rho_u$). Indeed for low χ values, $\chi < 0.1$ (very small quark concentrations), we can get α^Q values slightly larger than 1. However, we are cautious about these results since we can also expect some numerical problems. In fact, for very small χ values the weight of the α^Q contribution in the minimization procedure is not expected to be too relevant, as we can clearly see from Eq. (8). In any case the important point is that this is not affecting the general discussion about the isospin distillation.

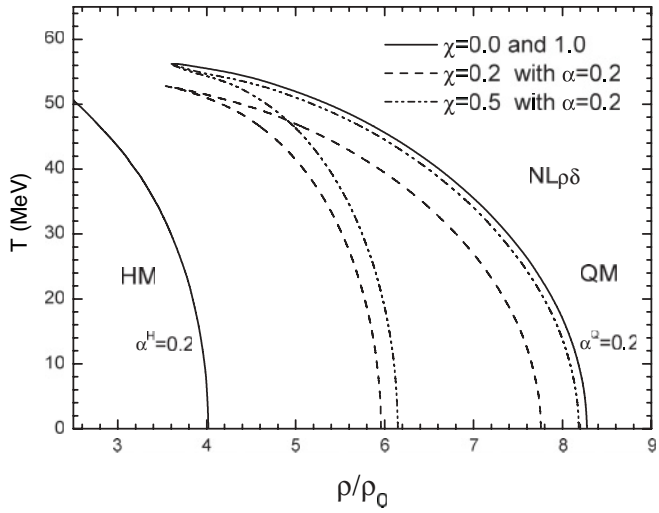

FIG. 9. Same as in Fig. 8, but for the NL$\rho\delta$ effective interaction in the hadron sector.

the effective N/Z of the quark phase in a 20% concentration. In the case of Au + Au (initial $N/Z = 1.5$) central collisions at 1 A GeV in pure hadronic simulations we get in the high-density phase a reduced $N/Z \sim 1.2$–1.25 (respectively, with NL$\rho\delta$-NLρ interactions) due to fast neutron emission [30,31]. The corresponding isospin content of the quark phases is much larger, $N/Z = 3.0$ for NLρ and $N/Z = 5.7$ for NL$\rho\delta$. This is the *neutron trapping* effect discussed in Sec. V. We would expect a signal of such large asymmetries, coupled to a larger baryon density in the quark phase, in the subsequent hadronization.

We finally remark that at higher temperature and smaller baryon chemical potential (ultrarelativistic collisions) the isospin effects discussed here are going to vanish [36], even if other physics can enter the game and charge asymmetry effects are predicted also at $\mu_B = 0$ and $T \simeq 170$ MeV [37,38].

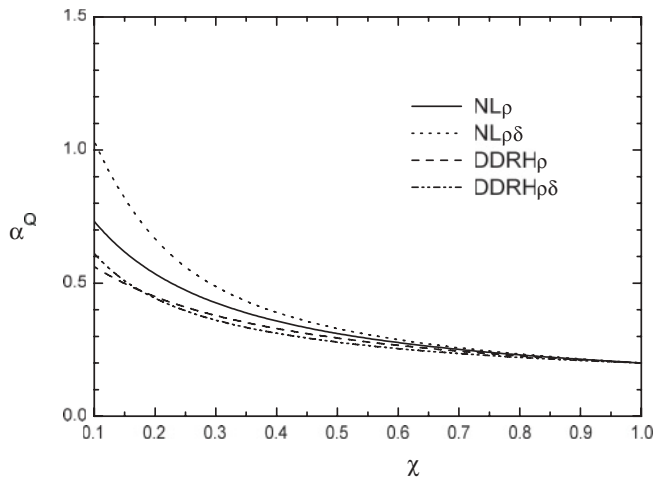

FIG. 10. Quark asymmetry in the mixed phase vs the quark concentration for asymmetric matter with $T = 0$ and $\alpha = 0.2$. NLρ and NL$\rho\delta$ effective hadron interactions are considered. The corresponding results with density-dependent couplings are also shown. Quark EoS: MIT bag model with $B^{1/4} = 160$ MeV.

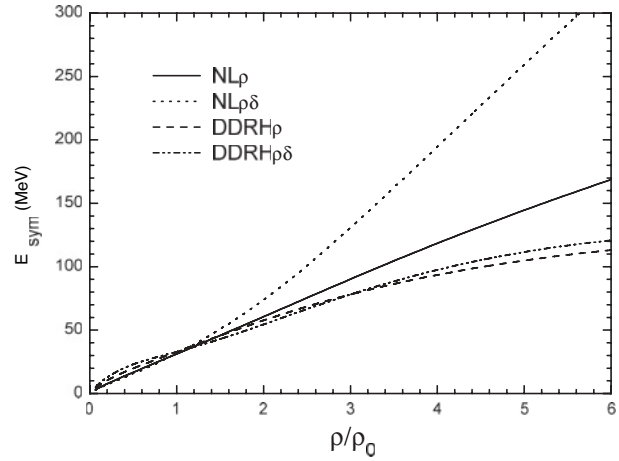

FIG. 11. Density dependence of the symmetry energy for the RMF hadron effective models used. NLρ and NL$\rho\delta$ represent the nonlinear effective hadron interactions with constant couplings. The corresponding results with density-dependent couplings are also shown.

In order to account for the the present uncertainties on our knowledge of the symmetry term of the hadron EoS at high baryon density (see also [16]) we have performed a new calculation using a RMF hadron interaction which gives a much softer behavior of the symmetry energy at high densities. In this way we can check the "robustness" of the expected isospin effects on the mixed phase discussed before. We use a density-dependent relativistic hadron (DDRH) field approach, where an explicit density dependence of the meson-nucleon couplings is introduced [39–41] (see details in Appendix A2). As clearly shown in Fig. 11, the main difference with respect to the previously presented results is that the symmetry energy is now less repulsive at high density. This is because, following some indications from Dirac-Brueckner calculations [42,43],

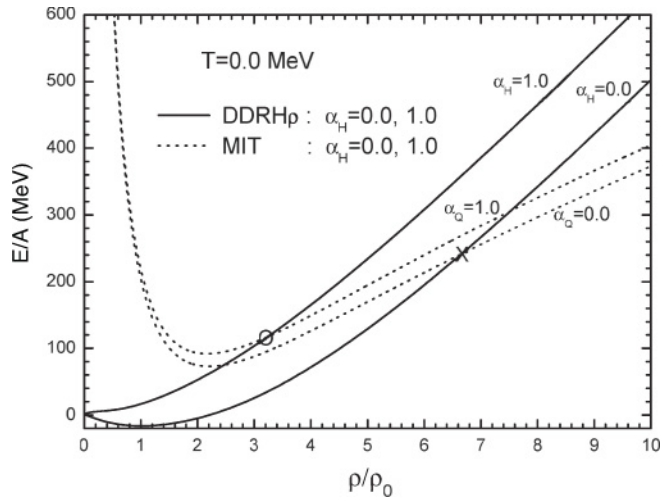

FIG. 12. Zero-temperature EoS of symmetric neutron matter: hadron (DDRHρ; solid lines) vs quark (MIT bag; dashed lines). $\alpha_{H,Q}$ represent the isospin asymmetry parameters of, respectively, the hadron and quark matter: $\alpha_{H,Q} = 0$, symmetric matter; $\alpha_{H,Q} = 1$, neutron matter.

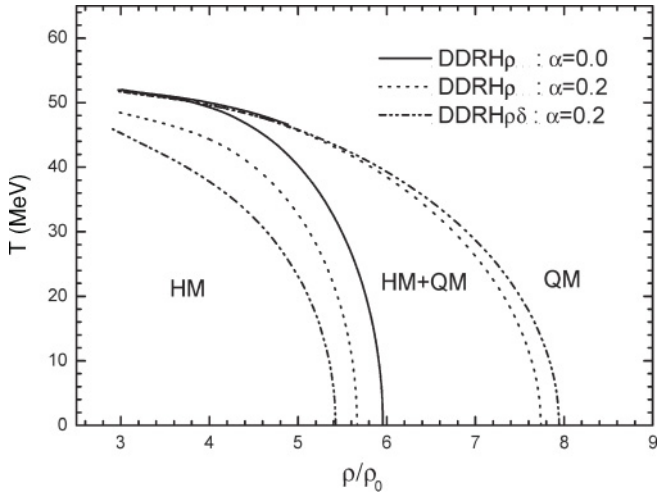

FIG. 13. Binodal surface for symmetric ($\alpha = 0.0$) and asymmetric ($\alpha = 0.2$) matter. Hadron EoS from DDRH interactions. Quark EoS: MIT bag model with $B^{1/4} = 160$ MeV.

the isovector-meson couplings in the DDRHρ and DDRH$\rho\delta$ cases show an increase for the attractive δ field and a decrease for the repulsive ρ field (see Fig. 14 in Appendix A2).

Moreover, interesting rearrangement terms are now present in the pressure and in the baryon chemical potentials, proportional to the density slopes of the couplings (see Appendix A2) and so particularly important at high densities, as also shown in neutron star applications [44].

We present first some results on the shift to lower densities of the onset of the mixed phase with increasing isospin asymmetry. In Fig. 12 we have the result with DDRHρ supporting the crossing argument of Fig. 1. Figure 13 shows in more detail the shift to the left of the lower boundaries. The curves should be compared to the corresponding lines of the NL constant-coupling model: DDRH to the solid lines of Fig. 3 (NL, $\alpha = 0.0$), DDRHρ to the solid lines of Fig. 6 (NLρ, $\alpha = 0.2$), and finally DDRH$\rho\delta$ to the solid lines of Fig. 7 (NL$\rho\delta$, $\alpha = 0.2$). We see that the isospin effects of the hadron-quark transition are still present, although with some reduction.

Finally, the new isospin distillation effects are shown as the DDRH results added in Fig. 10, about the isospin asymmetry in the quark phase for different quark concentrations. We note that for 20%–30% quark components we still see a noticeable increase of the isospin asymmetry.

We can conclude that the revealed isospin asymmetry effects on the hadron-quark mixed phase at high baryon density appear to be rather robust' with respect to relatively large variations of the stiffness of the symmetry term.

V. ISOSPIN IN EFFECTIVE QUARK MODELS

All these results will also be sensitive to the explicit inclusion of isovector interactions in effective nonperturbative QCD models at high baryon chemical potentials. Unfortunately, few attempts have been worked out for two main reasons: (i) the difficulties of lattice-QCD calculations at high baryon densities and (ii) the main interest on the QGP phase transition at high temperature and small baryon chemical potentials, as probed in the expanding fireball of ultrarelativistic heavy-ion collisions. A first approach can be supplied by a two-flavor NJL model [19], which in fact describes the chiral restoration but not the deconfinement dynamics. The isospin asymmetry can be included in a flavor-mixing picture [20,45], corresponding to different couplings to the (u, d) quark-antiquark condensates. As a consequence we can have now a dependence of the constituent mass of a given flavor to both quark condensates. We devote Appendix B to a detailed study of these isospin effects in the NJL chiral dynamics.

Due to the scalar nature of the interacting part of the corresponding Lagrangians only the quark effective mass dynamics will be affected. In the "realistic" small-mixing case (see also [45,46]), we get definite $M_u^* > M_d^*$ splitting at high baryon density (before the chiral restoration).

Taken together, these results can indicate a more fundamental confirmation of the $m_p^* > m_n^*$ splitting in the hadron phase, as suggested by the effective QHD model with the isovector scalar δ coupling (see [12,23]). However, such isospin mixing effect results in a very small variation of the symmetry energy in the quark phase, related only to the Fermi kinetic contribution. Moreover, recall that confinement is still missing in this NJL mean-field approach. In any case there are extensive suggestions about a favored chiral symmetry restoration in systems with large neutron excess [48].

More generally, starting from the QCD Lagrangian one can arrive to an effective color current-current interaction where an expansion in various components can provide isovector contributions, [49].

In this respect we remark on another interesting indirect isospin effect, i.e., not directly coming from isovector terms in the effective Lagrangian, but related to the presence of quark condensates due to the attractive gluon interaction. We note that just a color-pairing mechanism in the two-flavor system (the 2SC phase [50]) would imply a stiffer symmetry energy in the quark EoS since we have a larger attraction when the densities of up and down quarks are equal. An initial study of the high-density hadron-quark transition including such gluon correlations in the bag model has been presented very recently [21]. Now the symmetry energy difference between hadron and quark phases is partially reduced, at least at low temperatures, and consequently also the isospin effects discussed in detail in this work will be weaker, although still present. An interesting point is that in any case the quark phase is more bound due to the attractive gluon contribution. Hence the transition to the mixed phase will still appear at relatively low baryon densities, now for an "isoscalar" mechanism, within the reach of "low-energy" heavy-ion collisions, i.e., in the range of few A GeV. As an intuitive picture we can refer again to Fig. 1. Essentially the difference between the $\alpha_Q = 0.0$ and $\alpha_Q = 1$ curves is increasing but meanwhile both are decreasing.

With increasing temperature the color pairing effect will be in general reduced, as confirmed in [51] in an extended NJL calculation, and so isospin effects, as discussed before, will be more relevant. All this is naturally related to the chosen value of the superconducting gap, opening new stimulating perspectives. In this sense new experiments on mixed phase properties observed with isospin asymmetric

heavy-ion collisions, as suggested in the final section, will be extremely important.

VI. PERSPECTIVES AND SUGGESTED OBSERVABLES

Based on the qualitative argument of Sec. I and on more detailed calculations in a first-order phase transition scheme, we have predicted rather robust isospin effects on the hadron-quark transition at high baryon densities: these effects do not depend on details of the EoS parametrizations in the hadron and quark phases.

Our results seem to indicate a specific region where the onset of the mixed phase should be mainly located: $2 < \rho_B/\rho_0 < 4$, $T \leqslant 50$–60 MeV, for realistic asymmetries $\alpha \sim 0.2$–0.3. A key question is whether such a region of phase space can be explored by means of heavy-ion collisions. In Refs. [2,3] it is shown that even collisions of stable nuclei at intermediate energies ($E/A \sim 1$–2 GeV) make available the pertinent (T, ρ_B, α) region where the phase transition is expected to occur.

In this respect we can refer to the reaction $^{238}\mathrm{U} + ^{238}\mathrm{U}$ (average isospin asymmetry $\alpha = 0.22$) at 1 A GeV that has been investigated in Ref. [2], using a consistent relativistic mean-field approach with the same interactions, for a semi-central impact parameter $b = 7$ fm, chosen just to increase the neutron excess in the interacting region. The evolution of momentum distribution and baryon and isospin densities in a space cell located in the center of mass of the system has also been studied. After about 10 fm/c a local equilibration is achieved still in the compressed phase, before the fast expansion. We have a unique Fermi distribution and from a simple fit the "local" temperature can be evaluated. A rather exotic nuclear matter is formed in a transient time of the order of 10–20 fm/c, with baryon density around 3–4ρ_0, temperature 50–60 MeV, and isospin asymmetry between 0.2 and 0.3, likely inside the estimated mixed phase region.

Of course a relatively higher beam energy will allow entrance more deeply into the mixed phase. Such energies will however be available in the near future. In particular we notice that high-intensity ^{238}U beams in this energy range would be delivered in the first stage of the FAIR facility [4,52] and also at JINR-Dubna in the Nuclotron first step of the NICA project [36].

Which are the observable effects to look at if we enter and/or cross the mixed phase?

As already stressed, a first expectation will be the isospin distillation effect, a kind of *neutron trapping* in the quark phase, supported by statistical fluctuations [2] as well as by a symmetry energy difference in the two phases, as discussed in Sec. III. In fact, while in pure hadron matter (neutron-rich) at high density we have a large neutron potential repulsion (in both NLρ and NL$\rho\delta$ as well as in the corresponding DDRH cases), in the quark phase the d quarks see a smaller symmetry repulsion essentially only due to the kinetic contribution from the Fermi gas. As a consequence, while in a pure hadronic phase neutrons are quickly emitted or "transformed" in protons by inelastic collisions [31], when the mixed phase starts forming, neutrons are kept in the interacting system, in the quark phase, where they can even thermalize, up to the subsequent hadronization in the expansion stage [3]. Observables related to such neutron "trapping" could be the following:

(i) an inversion in the trend of emission of fast neutron-rich clusters with increasing beam energy, to be seen in the n/p and $^3\mathrm{H}/^3\mathrm{He}$ ratios at high kinetic energies;
(ii) an enhancement of the production of isospin-rich nucleon resonances and subsequent decays, which can be evaluated via equilibrium statistical approaches [53]; and
(iii) an increase of π^-/π^+ and K^0/K^+ yield ratios for mesons coming from high-density regions, to be selected via large transverse momenta, corresponding to a large radial flow.

If such kinetic selection of particles from the mixed phase can really be successful other potential signatures would also become available. One is related to the general softening of the matter, due to the contribution of more degrees of freedom that should show up in the damping of collective flows [54].

Azimuthal distributions (elliptic flows) will be particularly affected since particles mostly retain their high transverse momenta, escaping along directions orthogonal to the reaction plane without suffering much rescattering. Thus a further signature could be the observation, for the selected particles, of the onset of a quark-number scaling of the elliptic flow: a property of hadronization by quark coalescence that has been predicted and observed at RHIC energies, i.e., for the transition at $\mu_B = 0$ [55].

We note that all these results, on the binodal boundaries of the mixed phase and on the isospin distillation, are sensitive to the symmetry term in the hadron sector, although the main isospin effects are present for all the parametrizations of the isovector interaction. At variance, for the quark sector the lack of explicit isovector terms could strongly affect the location of the phase transition in asymmetric matter and the related expected observables.

In conclusion the aim of this work is twofold:

(i) to stimulate new experiments on isospin effects in heavy-ion collisions at intermediate energies (in a few A GeV range) with attention to the isospin content of produced particles and to elliptic flow properties, in particular for high-p_t selections, and
(ii) to stimulate more refined models of effective Lagrangians for nonperturbative QCD, where isovector channels are consistently accounted for and/or gluon correlations, leading to diquark condensates, can induce symmetry energy effects.

ACKNOWLEDGMENTS

This project is supported by the National Natural Science Foundation of China under Grant Nos. 10875160 and 11075037 and the INFN of Italy. This collaboration is supported in part by the Romanian Ministry for Education and Research under the CNCSIS contract PNII ID-946/2007. V.B. is grateful for the warm hospitality at Laboratori Nazionali del Sud, INFN.

APPENDIX A: EQUATION OF STATE FOR HADRONIC MATTER

1. Nonlinear relativistic mean-field model with constant couplings

A Lagrangian density with "minimal" meson channels and nonlinear terms is used. The nuclear interaction is mediated by two isoscalar, the scalar σ and the vector ω, and two isovector, the scalar δ and the vector ρ, mesons. Nonlinear terms are considered only for the σ contribution to account for the correct compressibility around saturation. Constant nucleon-meson couplings are used, chosen to reproduce the saturation properties and to represent a reasonable average of the density dependence predicted by relativistic Dirac-Brueckner-Hartree-Fock (DBHF) calculations [42,43] (see details in Refs. [12,23]):

$$\begin{aligned} L = {} & \bar{\psi}[i\gamma_\mu\partial^\mu - (M - g_\sigma\sigma - g_\delta\vec{\tau}\cdot\vec{\delta}) - g_\omega\gamma_\mu\omega^\mu \\ & - g_\rho\gamma^\mu\vec{\tau}\cdot\vec{b}_\mu]\psi + \tfrac{1}{2}\left(\partial_\mu\sigma\partial^\mu\sigma - m_\sigma^2\sigma^2\right) - U(\sigma) \\ & + \tfrac{1}{2}m_\omega^2\omega_\mu\omega^\mu + \tfrac{1}{2}m_\rho^2\vec{b}_\mu\cdot\vec{b}^\mu + \tfrac{1}{2}\left(\partial_\mu\vec{\delta}\cdot\partial^\mu\vec{\delta} - m_\delta^2\vec{\delta}^2\right) \\ & - \tfrac{1}{4}F_{\mu\nu}F^{\mu\nu} - \tfrac{1}{4}\vec{G}_{\mu\nu}\vec{G}^{\mu\nu}, \end{aligned} \tag{A1}$$

where $F_{\mu\nu} \equiv \partial_\mu\omega_\nu - \partial_\nu\omega_\mu$, $\vec{G}_{\mu\nu} \equiv \partial_\mu\vec{b}_\nu - \partial_\nu\vec{b}_\mu$, and the $U(\sigma)$ is the nonlinear potential of the σ meson: $U(\sigma) = \frac{1}{3}a\sigma^3 + \frac{1}{4}b\sigma^4$.

The EoS for nuclear matter at finite temperature in the mean-field approximation (RMF) is given by the energy density

$$\begin{aligned} \epsilon = {} & 2\sum_{i=n,p}\int\frac{d^3k}{(2\pi)^3}E_i^*(k)[f_i(k) + \bar{f}_i(k)] + \frac{1}{2}m_\sigma^2\sigma^2 + U(\sigma) \\ & + \frac{1}{2}\frac{g_\omega^2}{m_\omega^2}\rho_B^2 + \frac{1}{2}\frac{g_\rho^2}{m_\rho^2}\rho_3^2 + \frac{1}{2}\frac{g_\delta^2}{m_\delta^2}\rho_{s3}^2 \end{aligned} \tag{A2}$$

and pressure

$$\begin{aligned} p = {} & \frac{2}{3}\sum_{i=n,p}\int\frac{d^3k}{(2\pi)^3}\frac{k^2}{E_i^*(k)}[f_i(k) + \bar{f}_i(k)] - \frac{1}{2}m_\sigma^2\phi^2 - U(\phi) \\ & + \frac{1}{2}\frac{g_\omega^2}{m_\omega^2}\rho_B^2 + \frac{1}{2}\frac{g_\rho^2}{m_\rho^2}\rho_3^2 + \frac{1}{2}\frac{g_\delta^2}{m_\delta^2}\rho_{s3}^2, \end{aligned} \tag{A3}$$

where $E_i^* = \sqrt{k^2 + M_i^{*2}}$. The nucleon effective masses are defined as

$$M_i^* = M - g_\sigma\sigma \mp g_\delta\delta_3 \,(-\text{ for protons and} + \text{for neutrons}). \tag{A4}$$

The field equations in the RMF approach are

$$\sigma = -\frac{a}{m_\sigma^2}\sigma^2 - \frac{b}{m_\sigma^2}\sigma^3 + \frac{g_\sigma}{m_\sigma^2}(\rho_{sp} + \rho_{sn}), \tag{A5}$$

$$\omega_0 = \frac{g_\omega}{m_\omega^2}\rho, \tag{A6}$$

$$b_0 = \frac{g_\rho}{m_\rho^2}\rho_3, \tag{A7}$$

$$\delta_3 = \frac{g_\delta}{m_\delta^2}(\rho_{sp} - \rho_{sn}), \tag{A8}$$

where the baryon density $\rho \equiv \rho_B^H = \rho_p + \rho_n$ and $\rho_3^H = \rho_p - \rho_n$, and ρ_{sp} and ρ_{sn} are the scalar densities for the proton and the neutron, respectively. The $f_i(k)$ and $\bar{f}_i(k)$ in Eqs. (A2) and (A3) are the fermion and antifermion distribution functions for protons and neutrons ($i = p, n$):

$$f_i(k) = \frac{1}{1 + \exp\{(E_i^*(k) - \mu_i^*)/T\}}, \tag{A9}$$

$$\bar{f}_i(k) = \frac{1}{1 + \exp\{(E_i^*(k) + \mu_i^*)/T\}}, \tag{A10}$$

where the effective chemical potentials μ_i^* are determined by the nucleon densities

$$\rho_i = 2\int\frac{d^3k}{(2\pi)^3}[f_i(k) - \bar{f}_i(k)], \tag{A11}$$

while the scalar densities $\rho_{s,i}$, which give the coupling to the scalar fields, are given by

$$\rho_{s,i} = 2\int\frac{d^3k}{(2\pi)^3}\frac{M_i^*}{E_i^*}[f_i(k) + \bar{f}_i(k)]. \tag{A12}$$

(Note the M_i^*/E_i^* quenching factor at high baryon density.) Clearly at zero temperature the μ_i^* reduce to the in-medium Fermi energies $E_i{}^* = \sqrt{k^2 + M_i^{*2}}$.

The μ_i^* are related to the chemical potentials $\mu_i = \partial\epsilon/\partial\rho_i$ in terms of the vector meson mean fields by the equation

$$\begin{aligned} & \mu_i = \mu_i^* + \frac{g_\omega^2}{m_\omega^2}\rho \mp \frac{g_\rho^2}{m_\rho^2}\rho_3 \\ & (i = n, p : - \text{ for neutrons and} + \text{ for protons}) \end{aligned} \tag{A13}$$

The baryon and isospin chemical potentials in the hadron phase can be expressed in terms of the (p, n) ones as

$$\mu_B^H = \frac{\mu_p + \mu_n}{2}, \quad \mu_3^H = \frac{\mu_p - \mu_n}{2}. \tag{A14}$$

In the presence of the coupling to the two isovector ρ- and δ-meson fields, the expression for the symmetry energy has a simple transparent form (see [12,23,56]):

$$E_{\rm sym}(\rho) = \frac{1}{6}\frac{k_F^2}{E_F^*} + \frac{1}{2}\left[f_\rho - f_\delta\left(\frac{M^*}{E_F^*}\right)^2\right]\rho, \tag{A15}$$

where $M^* = M - g_\sigma\sigma$ and $E_F^* = \sqrt{k_F^2 + M^{*2}}$.

Now we easily see that in the NL$\rho\delta$ choice we have a large increase of the symmetry energy at high baryon densities. The potential symmetry term is given by the combination $[f_\rho - f_\delta(M^*/E_F^*)^2]$ of the repulsive vector ρ and attractive scalar δ isovector couplings. Thus, when the δ coupling is included we have to increase the ρ-meson coupling in order to reproduce the same asymmetry parameter a_4 at saturation. The net effect will be a stiffer symmetry energy at higher baryon densities due to the M^*/E_F^* quenching of the attractive part. Of course this mechanism can be largely modified if some density dependence is explicitly included in the meson-nucleon couplings, as we will see in the DDRH forces (Appendix A2), also used in this paper.

The coupling constants are fixed from good saturation properties and from averaged Dirac-Brueckner-Hartree-Fock

TABLE I. Parameter sets.

Parameter set	NLρ	NL$\rho\delta$
f_σ (fm^2)	10.32 924	10.32 924
f_ω (fm^2)	5.42 341	5.42 341
f_ρ (fm^2)	0.94 999	3.1500
f_δ (fm^2)	0.000	2.500
A (fm^{-1})	0.03 302	0.03 302
B	−0.00 483	−0.00 483

estimations (see the detailed discussions in Refs. [12,23,56]). DBHF indications of a density dependence of the meson-nucleon couplings at high baryon densities will be accounted for in the DDRH forces of Sec. A2.

The isoscalar part of the EoS is chosen to be rather soft at high densities (see [57]) in order to satisfy the experimental constraints from collective flows and kaon production in intermediate-energy heavy-ion collisions [25,26].

The coupling constants $f_i \equiv g_i^2/m_i^2, i = \sigma, \omega, \rho, \delta$, and the two parameters of the σ self-interacting terms, $A \equiv a/g_\sigma^3$ and $B \equiv b/g_\sigma^4$, are reported in Table I. The σ mass is fixed at 550 MeV. The corresponding properties of nuclear matter are listed in Table II. Here the binding energy is defined as $E/A = \epsilon/\rho - M$.

We finally note that these Lagrangians have already been used for flow [29], pion production [30], isospin tracer [58], and kaon production [31] calculations for relativistic heavy-ion collisions with an overall good agreement to data.

2. DDRH forces: Relativistic mean-field model with density-dependent couplings

The "minimal" Lagrangian density has the same form of Eq. (A1), now with density-dependent couplings and of course without nonlinear terms [the $U(\sigma)$ potential]. Apart from the effect of an explicit variation of the meson-nucleon couplings with baryon density we will expect new terms in the variational derivative of the Lagrangian density, the rearrangement terms Σ_μ^R that will affect the nucleon field equation, as well as the energy-momentum tensor, and so the EoS and the nucleon chemical potentials (see [39,40,44]). The nucleon field equation in a mean-field approximation (RMF) is

$$\left[i\gamma_\mu\partial^\mu - (M - g_\sigma\sigma - g_\delta\tau_3\delta_3) - g_\omega\gamma^0\omega_0 - g_\rho\gamma^0\tau_3 b_0 + \gamma^0\Sigma_0^R\right]\psi = 0 \tag{A16}$$

TABLE II. Saturation properties of nuclear matter.

ρ_0 (fm^{-3})	0.16
E/A (MeV)	−16.0
K (MeV)	240.0
$E_{\rm sym}$ (MeV)	31.3
M^*/M	0.75

with

$$\begin{aligned}
\sigma &= \frac{g_\sigma}{m_\sigma^2}\rho_s = \frac{g_\sigma}{m_\sigma^2}(\rho_{sp} + \rho_{sn}),\\
\omega_0 &= \frac{g_\omega}{m_\omega^2}\langle\bar\psi\gamma^0\psi\rangle = \frac{g_\omega}{m_\omega^2}\rho = \frac{g_\omega}{m_\omega^2}(\rho_p + \rho_n),\\
b_0 &= \frac{g_\rho}{m_\rho^2}\langle\bar\psi\gamma^0\tau_3\psi\rangle = \frac{g_\rho}{m_\rho^2}\rho_3,\\
\delta_3 &= \frac{g_\delta}{m_\delta^2}\langle\bar\psi\tau_3\psi\rangle = \frac{g_\delta}{m_\delta^2}\rho_{s3}
\end{aligned} \tag{A17}$$

and the rearrangement term

$$\Sigma_0^R = \left(\frac{\partial g_\sigma}{\partial\rho}\right)\frac{g_\sigma}{m_\sigma^2}\rho_s + \left(\frac{\partial g_\delta}{\partial\rho}\right)\frac{g_\delta}{m_\delta^2}\rho_{s3}^2 - \left(\frac{\partial g_\omega}{\partial\rho}\right)\frac{g_\omega}{m_\omega^2}\rho^2 - \left(\frac{\partial g_\rho}{\partial\rho}\right)\frac{g_\rho}{m_\rho^2}\rho_3^2, \tag{A18}$$

where $\rho_3 = \rho_p - \rho_n$ and $\rho_{s3} = \rho_{sp} - \rho_{sn}$, with ρ_i, ρ_{si} $(i = n, p)$ the nucleon and the scalar densities (see Sec. A1).

Neglecting the derivatives of meson fields, we have that the energy-momentum tensor in RMF approximation is given by

$$T_{\mu\nu} = i\bar\psi\gamma_\mu\partial_\nu\psi + \left[\tfrac{1}{2}m_\sigma^2\sigma^2 - \tfrac{1}{2}m_\omega^2\omega_\lambda\omega^\lambda - \tfrac{1}{2}m_\rho^2\vec b_\lambda\vec b^\lambda + \tfrac{1}{2}m_\delta^2\vec\delta^2 + \bar\psi\Sigma_\lambda^R\gamma^\lambda\psi\right]g_{\mu\nu}. \tag{A19}$$

The equation of state for nuclear matter at finite temperature can be obtained from the thermodynamic potential. Using the meson field equations (A17), the energy density has the form

$$\epsilon = \sum_{i=n,p} 2\int\frac{d^3k}{(2\pi)^3}E_i^*(k)[f_i(k) + \bar f_i(k)] + \frac{1}{2}\frac{g_\sigma^2}{m_\sigma^2}\rho_s^2 + \frac{1}{2}\frac{g_\omega^2}{m_\omega^2}\rho^2 + \frac{1}{2}\frac{g_\rho^2}{m_\rho^2}\rho_3^2 + \frac{1}{2}\frac{g_\delta^2}{m_\delta^2}\rho_{s3}^2, \tag{A20}$$

and the pressure is

$$p = \sum_{i=n,p}\frac{2}{3}\int\frac{d^3k}{(2\pi)^3}\frac{k^2}{E_i^*(k)}\left[f_i(k) + \bar f_i(k)\right] - \frac{1}{2}\frac{g_\sigma^2}{m_\sigma^2}\rho_s^2 + \frac{1}{2}\frac{g_\omega^2}{m_\omega^2}\rho^2 + \frac{1}{2}\frac{g_\rho^2}{m_\rho^2}\rho_3^2 - \frac{1}{2}\frac{g_\delta^2}{m_\delta^2}\rho_{s3}^2 - \Sigma_o^R\rho. \tag{A21}$$

The nucleon chemical potentials μ_i are given in terms of the vector meson mean fields as in the constant-coupling case [Eq. (A13)] apart the new rearrangement term

$$\mu_i = \mu_i^* + \frac{g_\omega^2}{m_\omega^2}\rho \mp \frac{g_\rho^2}{m_\rho^2}\rho_3 - \Sigma_o^R \quad (i = n, p : - \text{ for neutrons and } + \text{ for protons}) \tag{A22}$$

with the effective masses related to the scalar fields as before:

$$M_i^* = M - \frac{g_\sigma^2}{m_\sigma^2}\rho_s^2 \mp \frac{g_\delta^2}{m_\delta^2}\rho_{s3}^2 \quad (i = n, p : + \text{ for neutrons and } - \text{ for protons}). \tag{A23}$$

A general form of parametrization for the density dependence of the meson-nucleon couplings can be given by

$$g_i(\rho) = g_i(\rho_0)f_i(x), \quad \text{for} \quad i = \sigma, \omega, \rho, \delta, \tag{A24}$$

TABLE III. DDRH parameters.

Model	DDRH		DDRHρ	DDRH$\rho\delta$	
	σ	ω	ρ	ρ	δ
m_i (MeV)	550	783	770	770	980
g_i (ρ_0)	10.73	13.29	3.59	6.48	7.59
a_i	1.37	1.40	0.095	0.095	0.02
b_i	0.23	0.17	2.17	2.17	3.47
c_i	0.41	0.34	0.05	0.05	−0.09
d_i	0.90	0.98	17.84	17.84	−9.81

with $x = \rho/\rho_0$ and ρ_0 the saturation density. As already mentioned the $f_i(x)$ are chosen in order to reproduce the density dependence of the couplings deduced from microscopic DBHF calculations. For symmetric matter this analysis has been performed in Ref. [40] using for the isoscalar mesons a functional of the form

$$f_i(x) = a_i \frac{1 + b_i(x + d_i)^2}{1 + c_i(x + d_i)^2}, \quad \text{for } i = \sigma, \omega, \tag{A25}$$

In the case of asymmetric matter the following parametrization has been proposed for the isovector couplings [41]:

$$f_i(x) = a_i \exp[-b_i(x - 1)] - c_i(x - d_i), \quad \text{for } i = \rho, \delta. \tag{A26}$$

In this way it easier to reproduce the important difference of the δ and ρ couplings at high density.

The parametrization form and parameters of our DDRH forces are taken from Ref. [40] for σ and ω mesons and from Ref. [41] for ρ and δ mesons, respectively. All parameters are listed in Table III. The density-dependent couplings as a function of baryon density are displayed in Fig. 14.

The choice of the $g_i(\rho_0)$ couplings at saturation is performed in order to have the same normal nuclear matter properties of the nonlinear RMF models (Table II) of Sec. A1. The EoS of symmetric matter at high density is also not affected, as we can see by comparing the binodal surfaces for zero asymmetry of Figs. 3 and 13 (solid lines).

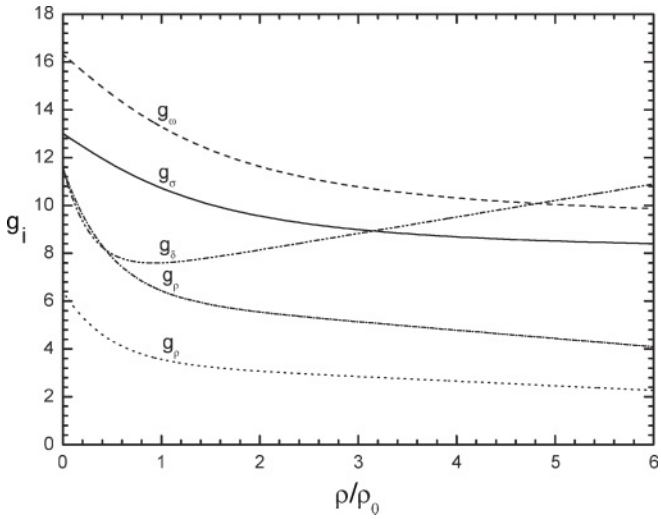

FIG. 14. Density dependence of the meson-nucleon couplings in the DDRH interactions used. The g_ρ dotted line at the bottom corresponds to the DDRHρ case, without the δ meson.

At variance, the different behaviors of the isovector couplings at high density, increase of g_δ and decrease of g_ρ, will contribute to get a much softer symmetry energy at high baryon densities (Fig. 11). It is easy to check that in this way in nucleonic models of neutron stars the proton fraction limit for the onset of direct URCA processes is hardly reached (see the analysis of Ref. [59]). For the purpose of the present paper the use of DDRH interactions is important in order to show that the expected isospin effects on the mixed phase are present even with much softer symmetry terms at high baryon densities.

APPENDIX B: NAMBU–JONA-LASINIO MODEL FOR ASYMMETRIC MATTER

From the previous discussion it appears (extremely) important to include the isospin degree of freedom in any effective QCD dynamics. A first approach can be supplied by a two-flavor Nambu–Jona-Lasinio model where the isospin asymmetry can be included in a flavor-mixing picture [20,45]. The Lagrangian is given by

$$L = L_0 + L_1 + L_2, \tag{B1}$$

with L_0 the free part,

$$L_0 = \bar{\psi}(i\ \partial\!\!\!/ - m)\psi,$$

and the two different interaction parts given by

$$\begin{aligned} L_1 &= G_1\{(\bar{\psi}\psi)^2 + (\bar{\psi}\vec{\tau}\psi)^2 + (\bar{\psi}i\gamma_5\psi)^2 + (\bar{\psi}i\gamma_5\vec{\tau}\psi)^2\}, \\ L_2 &= G_2\{(\bar{\psi}\psi)^2 - (\bar{\psi}\vec{\tau}\psi)^2 - (\bar{\psi}i\gamma_5\psi)^2 + (\bar{\psi}i\gamma_5\vec{\tau}\psi)^2\}. \end{aligned} \tag{B2}$$

In the mean-field approximation the new gap equations are $M_i = m_i - 4G_1\Phi_i - 4G_2\Phi_j, i \neq j, (u, d)$, where the $\Phi_{u,d} = \langle\bar{u}u\rangle, \langle\bar{d}d\rangle$ are the two (negative) condensates, which are given by

$$\Phi_f = -2N_c \int \frac{d^3p}{(2\pi)^3} \frac{M_f}{E_{p,f}} \{1 - f^-(T, \mu_f) - f^+(T, \mu_f)\}, \tag{B3}$$

and $m_{u,d} = m$ are the (equal) current masses.

Introducing explicitly a flavor mixing, i.e., the dependence of the constituent mass of a given flavor to both condensate, via $G_1 = (1 - \beta)G_0$, $G_2 = \beta G_0$, we have the coupled equations

$$\begin{aligned} M_u &= m - 4G_0\Phi_u + 4\beta G_0(\Phi_u - \Phi_d), \\ M_d &= m - 4G_0\Phi_u + 4(1 - \beta)G_0(\Phi_u - \Phi_d). \end{aligned} \tag{B4}$$

For $\beta = 1/2$ we get the usual NJL ($M_u = M_d$), while small or large mixing is for $\beta \Rightarrow 0$ or $\beta \Rightarrow 1$, respectively. The value of β has a consequence on the structure of the phase diagram in the region of low temperatures and high chemical potential. In fact, as shown in [20,45], for $\beta = 0$ there are two distinct phase transitions for the up quarks and for the down quarks, but for this value the interaction is symmetric under $U_A(1)$ transformations and it is unrealistic. While for $\beta \geqslant 0.1$ the $U_A(1)$ symmetry becomes explicitly broken and

there is only a single first-order phase transition. Realistic estimations of β fitting the physical η-meson mass give a value of $\beta \approx 0.11$ [45,46].

In neutron-rich matter $|\Phi_d|$ decreases more rapidly due to the larger ρ_d and so $(\Phi_u - \Phi_d) < 0$. In the "realistic" small-mixing case we will get a definite $M_u > M_d$ splitting at high baryon density (before the chiral restoration). This expectation is confirmed by a full calculation of the coupled gap equations with standard parameters [3,47]. All this can indicate a more fundamental confirmation of the $m_p^* > m_n^*$ splitting in the hadron phase, as suggested by the effective QHD model with the isovector scalar δ coupling (see [12,23]).

However, such an isospin mixing effect results in a very small variation of the symmetry energy in the quark phase, still related only to the Fermi kinetic contribution. In fact, this represents just a very first step toward a more complete treatment of isovector contributions in effective quark models, of large interest for the discussion of the phase transition at high densities.

[1] H. Müller, Nucl. Phys. A **618**, 349 (1997).
[2] M. Di Toro, A. Drago, T. Gaitanos, V. Greco, and A. Lavagno, Nucl. Phys. A **775**, 102 (2006).
[3] M. Di Toro *et al.*, Prog. Part. Nucl. Phys. **62**, 389–401 (2009).
[4] P. Senger *et al.*, J. Phys. G **36**, 064037 (2009).
[5] See [http://nica.jinr.ru/].
[6] G. F. Burgio, M. Baldo, P. K. Sahu, and H.-J. Schulze, Phys. Rev. C **66**, 025802 (2002).
[7] M. Bejger, P. Haensel, and J. L. Zdumik, Mon. Not. R. Astron. Soc. **359**, 699 (2005).
[8] O. E. Nicotra, M. Baldo, G. F. Burgio, and H.-J. Schulze, Phys. Rev. D **74**, 123001 (2006).
[9] M. Baldo, G. F. Burgio, P. Castorina, S. Plumari, and D. Zappala, Phys. Rev. C **66**, 035804 (2007).
[10] G. F. Burgio, and S. Plumari, Phys. Rev. D **77**, 085022 (2008).
[11] A. Rahbi, H. Pais, P. K. Panda, and C. Procidencia, arXiv:0909.1114 [nucl-th].
[12] V. Baran, M. Colonna, V. Greco, and M. Di Toro, Phys. Rep. **410**, 335 (2005).
[13] C. Fuchs and H. H. Wolter, Eur. Phys. J. A **30**, 5 (2006).
[14] B. A. Li, L. W. Chen, and C. M. Ko, Phys. Rep. **465**, 113 (2008).
[15] W. Trautmann, Nucl. Phys. A **834**, 548c (2010); arXiv:1001.3867 [nucl-exp].
[16] V. Giordano, M. Colonna, M. Di Toro, V. Greco, and J. Rizzo, Phys. Rev. C **81**, 044611 (2010).
[17] M. Di Toro, V. Baran, M. Colonna, and V. Greco, J. Phys. G **37**, 083101 (2010).
[18] A. Chodos, R. L. Jaffe, K. Johnson, C. B. Thorn, and V. F. Weisskopf, Phys. Rev. D **9**, 3471 (1974).
[19] Y. Nambu and G. Jona-Lasinio, Phys. Rev. **122**, 345 (1961); **124** 246 (1961).
[20] M. Buballa, Phys. Rep. **407**, 205 (2005).
[21] G. Pagliara, J. Schaffner-Bielich, arXiv:1003.1017 [nucl-th].
[22] B. D. Serot and J. D. Walecka, Adv. Nucl. Phys. **16**, 1 (1986).
[23] B. Liu, V. Greco, V. Baran, M. Colonna, and M. Di Toro, Phys. Rev. C **65**, 045201 (2002).
[24] D. Page and S. Reddy, Annu. Rev. Nucl. Part. Sci. **56**, 327 (2006).
[25] P. Danielewicz, R. Lacey, and W. G. Lynch, Science **298**, 1592 (2002).
[26] C. Fuchs, Prog. Part. Nucl. Phys. **56**, 1 (2006).
[27] B. Müller, Rep. Prog. Phys. **58**, 611 (1995).
[28] L. D. Landau and L. Lifshitz, *Statistical Physics* (Pergamon, Oxford, 1969).
[29] V. Greco *et al.*, Phys. Lett. B **562**, 215 (2003).
[30] T. Gaitanos *et al.*, Nucl. Phys. A **732**, 24 (2004).
[31] G. Ferini, T. Gaitanos, M. Colonna, M. Di Toro, and H. H. Wolter, Phys. Rev. Lett. **97**, 202301 (2006).
[32] N. K. Glendenning and S. A. Moszkowski, Phys. Rev. Lett. **67**, 2414 (1991).
[33] D. Vretenar, T. Niksic, and P. Ring, Phys. Rev. C **68**, 024310 (2003), and references therein.
[34] V. Baran, M. Colonna, M. Di Toro, and A. Larionov, Nucl. Phys. A **632**, 287 (1998).
[35] P. Chomaz, M. Colonna, and J. Randrup. Phys. Rep. **389**, 263 (2004).
[36] A. N. Sissakian, A. S. Sorin, and V. D. Toneev, Phys. Part. Nucl. **39**, 1062 (2008).
[37] J. B. Kogut and D. K. Sinclair, Phys. Rev. D **70**, 094501 (2004).
[38] D. Toublan and J. B. Kogut, Phys. Lett. B **605**, 129 (2005).
[39] C. Fuchs, H. Lenske, and H. H. Wolter, Phys. Rev. C **52**, 3043 (1995).
[40] S. Typel and H. H. Wolter, Nucl. Phys. A **656**, 331 (1999).
[41] S. S. Avancini, L. Brito, D. P. Menezes, and C. Providencia, Phys. Rev. C **70**, 015203 (2004).
[42] F. Hofmann, C. M. Keil, and H. Lenske, Phys. Rev. C **64**, 034314 (2001).
[43] P. Goegelein, E. N. E. van Dalen, C. Fuchs, and H. Müther, Phys. Rev. C **77**, 025802 (2008).
[44] B. Liu *et al.*, Phys. Rev. C **75**, 048801 (2007).
[45] M. Frank, M. Buballa, and M. Oertel, Phys. Lett. B **562**, 221 (2003).
[46] G. Y. Shao, L. Chang, Y. X. Liu, and X. L. Wang, Phys. Rev. D **73**, 076003 (2006).
[47] S. Plumari, Ph.D. thesis, University of Catania, 2009.
[48] N. Kaiser and W. Weise, Phys. Lett. B **671**, 25 (2009).
[49] W. Weise, Prog. Theor. Phys. Suppl. **170**, 161 (2007).
[50] M. G. Alford, A. Schmitt, K. Rajagopal, and T. Schafer, Rev. Mod. Phys. **80**, 1455 (2008).
[51] M. Huang, P. Zhuang, and W. Chao, Phys. Rev. D **67**, 065015 (2003).
[52] H. Stöcker (private communication).
[53] G. Ferini, M. Colonna, T. Gaitanos, and M. Di Toro, Nucl. Phys. A **762**, 147 (2005).
[54] L. Csernai and D. Rohrich, Phys. Lett. B **458**, 454 (1999).
[55] R. J. Fries, V. Greco V, and P. Sörensen, Annu. Rev. Nucl. Part. Sci. **58**, 177 (2008).
[56] V. Greco, M. Colonna, M. Di Toro, and F. Matera, Phys. Rev. C **67**, 015203 (2003).
[57] B. Liu, H. Guo, M. Di Toro, and V. Greco, Eur. Phys. J. A **25**, 293 (2005).
[58] T. Gaitanos, M. Colonna, M. Di Toro, and H. H. Wolter, Phys. Lett. B **595**, 209 (2004).
[59] T. Klähn *et al.*, Phys. Rev. C **74**, 035802 (2006).